# **Accepted Manuscript**

# **Accepted Manuscript (Uncorrected Proof)**

**Title:** Neuroprotective Effects of Astaxanthin on Functional, Biochemical, and Histological Outcomes after Middle Cerebral Artery Occlusion Stroke in Male Rats: the CA1 Hippocampal Region

Running Title: Astaxanthin Neuroprotection in Stroke

**Authors:** Parsa Pourmohammadi<sup>1</sup>, Mobina Gheibi<sup>2,3</sup>, Sina Baghi Keshtan<sup>4</sup>, Erfan Ghadirzadeh<sup>3</sup>, Melika Pourhossein<sup>5</sup>, Ali Siahposht-Khachaki<sup>6,\*</sup>

- 1. Animal Research Center, Mazandaran University of Medical Sciences, Sari, Iran.
- Department of Laboratory Sciences, Razi Hospital, Mazandaran University of Medical Sciences,
   Qaemshahr, Iran.
- 3. Non-Communicable Diseases Institute, Mazandaran University of Medical Sciences, Sari, Iran.
- 4. School of Medicine, Birjand University of Medical Sciences, Birjand, Iran.
- 5. School of Pharmacy, Mazandaran University of Medical Sciences, Sari, Iran.
- 6. Immunogenetics Research Center, School of Medicine; Department of Physiology, Mazandaran University of Medical Sciences, Sari, Iran.

\*Corresponding Author: Ali Siahposht-Khachaki, Immunogenetics Research Center, School of Medicine; Department of Physiology, Mazandaran University of Medical Sciences, Sari, Iran.

Email: ak57n@yahoo.com, a.siahposht@mazums.ac.ir

To appear in: **Basic and Clinical Neuroscience** 

**Received date:** 2025/10/31

**Revised date:** 2025/11/05

**Accepted date:** 2025/11/07

This is a "Just Accepted" manuscript, which has been examined by the peer-review process and has been accepted for publication. A "Just Accepted" manuscript is published online shortly after its acceptance, which is prior to technical editing and formatting and author proofing. Basic and Clinical Neuroscience provides "Just Accepted" as an optional and free service which allows authors to make their results available to the research community as soon as possible after acceptance. After a manuscript has been technically edited and formatted, it will be removed from the "Just Accepted" Web site and published as a published article. Please note that technical editing may introduce minor changes to the manuscript text and/or graphics which may affect the content, and all legal disclaimers that apply to the journal pertain.

### Please cite this article as:

Pourmohammadi, P., Gheibi, M., Baghi Keshtan, S., Ghadirzadeh, E., Pourhossein, M., Siahposht-Khachaki, A. (In Press). Neuroprotective Effects of Astaxanthin on Functional, Biochemical, and Histological Outcomes after Middle Cerebral Artery Occlusion Stroke in Male Rats: the CA1 Hippocampal Region. Basic and Clinical Neuroscience. Just Accepted publication Jul. 10, 2025. Doi: http://dx.doi.org/10.32598/bcn.2025.7494.2

DOI: http://dx.doi.org/10.32598/bcn.2025.7494.2

### **Abstract**

**Background:** Ischemic stroke often results in severe neurological impairment, particularly affecting the hippocampal CA1 region, which is highly vulnerable to ischemia-reperfusion injury. Astaxanthin (ATX), a potent antioxidant carotenoid, has demonstrated some neuroprotective, anti-inflammatory, and anti-apoptotic properties. This study investigated the effects of ATX on functional, biochemical, and histological outcomes following focal transient middle cerebral artery occlusion (MCAO) model in rats.

Methods: Fifty-six male Wistar rats were randomly assigned to seven groups: Intact, Sham, Stroke (MCAO), Solvent (0.1% DMSO), and ATX-treated groups (25, 50, or 100 mg/kg, intraperitoneally every 12 hours for 3 days post-MCAO). Neurological function (bederson score), motor coordination (rotarod), spatial learning (morris water maze), and memory retention (passive avoidance learning using shuttle box) were assessed. Cerebrospinal fluid cytokine levels (IL-10, IL-1β), cerebral edema, and hippocampal CA1 histology were analyzed.

**Results:** Low (25 mg/kg) and medium (50 mg/kg) ATX doses significantly improved neurological and functional performance compared with untreated MCAO rats (P < 0.01). These doses increased IL-10 and reduced IL-1 $\beta$  levels, decreased brain water content, and preserved neuronal morphology in the CA1 region. Conversely, the high dose (100 mg/kg) conferred no significant benefit. Histopathology confirmed reduced neuronal damage and apoptosis at effective doses.

**Conclusion:** Post-ischemic ATX administration provides neuroprotection in a rat MCAO model, with 25–50 mg/kg yielding optimal outcomes. The observed inverted dose-response underscores the importance of precise dosing and timing. ATX represents a promising therapeutic candidate for ischemic stroke pending further translational studies.

Keywords: Astaxanthin, Middle Cerebral Artery Occlusion, Reperfusion Injury, Rat, Ischemic Stroke

# **Highlights**

- Astaxanthin at 25 and 50 mg/kg improved neurological function post-stroke.
- Low and medium doses reduced cerebral edema and neuroinflammation.
- Hippocampal CA1 neuronal structure was preserved by effective doses.
- A high dose (100 mg/kg) showed no neuroprotective benefits.

# **Plain Language Summary**

A stroke happens when the blood supply to part of the brain is cut off, which can cause lasting brain damage, disability, and problems with memory and movement. A specific part of the brain, called the hippocampus, is especially vulnerable to this damage. In this study, researchers investigated whether a natural substance called astaxanthin could protect the brain in the aftermath of a stroke. Astaxanthin is a powerful antioxidant found in seafood like salmon and in microalgae, and it is known for its anti-inflammatory properties. The study was conducted on male rats that had experienced an experimentally induced stroke. We treated the rats with different doses of astaxanthin after the stroke occurred. Then, we measured the rats' recovery, looking at their ability to move, learn, and remember, as well as brain swelling and inflammation. We found that rats given low and medium doses of astaxanthin (25 and 50 mg/kg) showed significant improvements. These animals had better memory and coordination, less brain swelling, and reduced inflammation. Their brain cells in the critical hippocampal region were also better preserved. Surprisingly, a higher dose (100 mg/kg) provided no benefit at all. This research matters because stroke is a leading cause of disability worldwide, and treatment options are limited. The findings suggest that astaxanthin could be a promising candidate for a new stroke therapy, helping to protect the brain from damage and improve recovery. However, the discovery that a higher dose was ineffective is a critical warning, it shows that "more is not always better." This emphasizes the need for careful future studies to determine the perfect dose and timing for treatment in humans, ensuring this potential therapy is both safe and effective.

# Introduction

Of all stroke types, ischemic stroke, triggered by a blockage in a cerebral blood vessels, is the most common and a major contributor to global mortality and disability (Saini et al., 2021). The middle cerebral artery (MCA) is frequently occluded in such events, often resulting in serious neurological impairment. A brain area especially susceptible to this damage is the CA1 region of the hippocampus, owing to its high metabolic rate and sensitivity to interruptions in oxygen and glucose (Liang et al., 2016; Zhu et al., 2012). This sensitivity can lead to significant cognitive and behavioral deficits, making the CA1 a key focus for research into neuroprotection after stroke. A paradoxical phenomenon known as ischemia-reperfusion injury can worsen cellular damage when blood flow is restored (for instance, by tissue plasminogen activator) (Jurcau & Ardelean, 2022). This process accelerates the formation of reactive oxygen species (ROS), leading to oxidative stress, mitochondrial dysfunction, and the activation of complex neurotoxic cascades involving excitotoxicity, inflammation, and apoptosis. The resulting neuroinflammation, driven by pro-inflammatory cytokines like TNF-α, IL-6, and IL-1β, disrupts the blood-brain barrier (BBB), exacerbates edema, and contributes to secondary neuronal death (Jurcau & Ardelean, 2022; Sun et al., 2018). Therefore, therapeutic agents that can simultaneously mitigate oxidative stress, inflammation, and apoptotic pathways are of immense interest (Lin et al., 2016; Mahyar et al., 2025).

Astaxanthin (ATX), a naturally occurring xanthophyll carotenoid found in microalgae and seafood, has emerged as a potent candidate. It is a powerful antioxidant, with a molecular structure that allows it to effectively quench free radicals and protect cell membranes. Beyond its antioxidant capacity, ATX has demonstrated significant anti-inflammatory and anti-apoptotic properties in various experimental models in liver, retina, and kidney ischemia-reperfusion injury (Li et al.,

2017; Otsuka et al., 2016; Qiu et al., 2015). Its neuroprotective potential has been observed in studies of global cerebral ischemia and subarachnoid hemorrhage, where it activates protective cellular pathways such as the Nrf2/ARE signaling cascade, leading to the upregulation of endogenous antioxidant enzymes like heme oxygenase-1 (HO-1) (Ashrafizadeh et al., 2022; Qian et al., 2021; Taheri et al., 2022; Xue et al., 2017; Yang et al., 2021; Yuguang et al., 2025). Critically, ATX is fat-soluble, enabling it to cross the BBB, and has an established safety profile with approval for use as a dietary supplement (Brendler & Williamson, 2019; Galasso et al., 2018; Grimmig et al., 2017).

However, despite these promising attributes, its specific effects on regional brain ischemia, particularly on the vulnerable hippocampal CA1 neurons following focal MCA occlusion (MCAO), remain insufficiently explored. The existing evidence highlights a need to elucidate the precise behavioral, biochemical, and histological outcomes associated with ATX treatment in a focal stroke model. Consequently, this research sought to determine whether ATX provides neuroprotection, specifically for hippocampal CA1 neurons, in an MCAO rat model by evaluation of its effects on functional recovery through behavioral tests, quantification of the modulation of key inflammatory markers (interleukins), and assessment of the preservation of neuronal structure through qualitative histopathological analysis.

# **Materials and Methods**

# Animals

This experiment utilized 56 male Albino-Wistar rats, weighing 250-300 g and aged 8-10 weeks. The animals were kept in a controlled environment with a 12-hour light/dark cycle, a temperature of 22-25°C, and unrestricted food and water. The Research Ethics Committee of Laboratory

Animals at Mazandaran University of Medical Sciences granted ethical approval for all procedures (IR.MAZUMS.AEC.1403.031). The study adhered to the ARRIVE guidelines, the university's ethical standards, and the UK's Animals (Scientific Procedures) Act 1986.

# Experimental groups

Figure 1 outlines a schematic of the study's experimental protocol. The rats were randomly divided into the following seven experimental groups (8 rats in each group):

- 1. Intact group: No interventions.
- 2. Sham group: Underwent surgery and anesthesia without MCAO induction.
- 3. Stroke group: MCAO was induced but received no medication or placebo.
- 4. Solvent group: MCAO + 0.1% DMSO (as solvent or placebo)
- 5. Low-dose group: MCAO + 25 mg/kg ATX
- 6. Medium-dose group: MCAO + 50 mg/kg ATX
- 7. High-dose group: MCAO + 100 mg/kg ATX

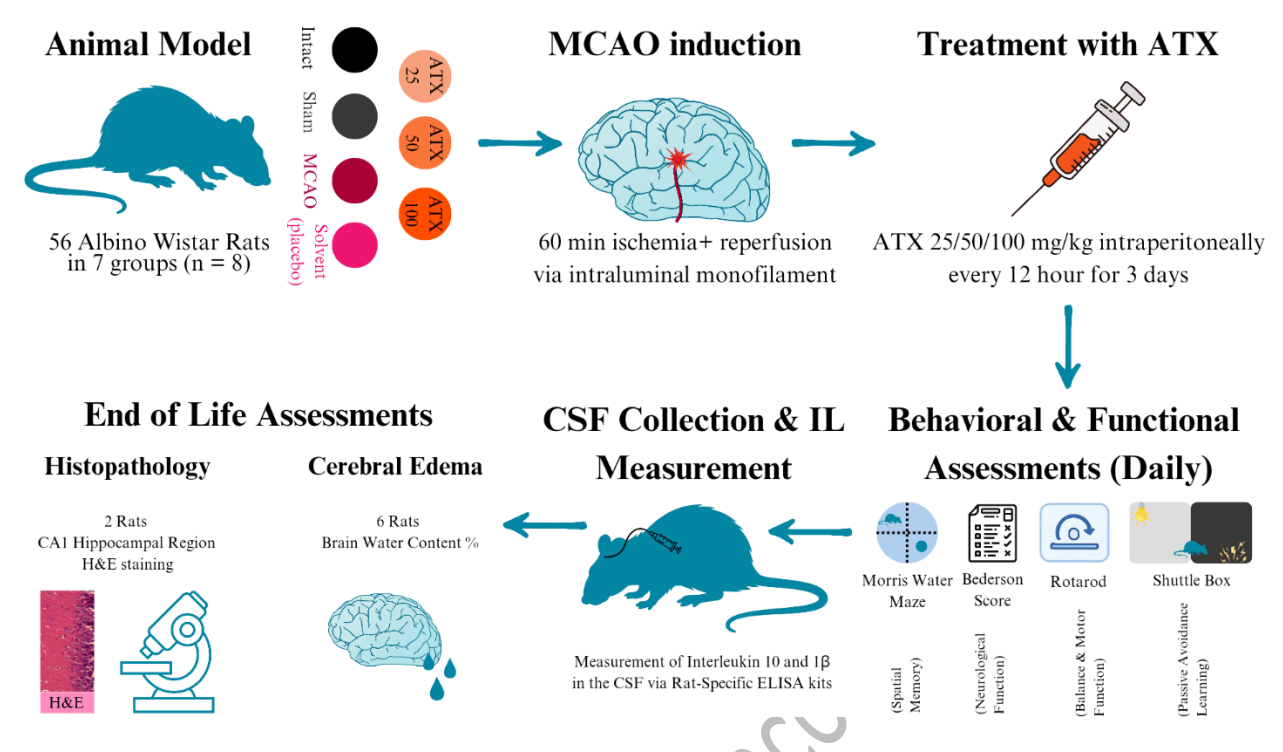


**Figure 1.** This schematic outlines the study's experimental protocol. Fifty-six male rats were randomly assigned to one of seven experimental groups. The Intact and Sham groups underwent neither stroke induction nor pharmacological intervention. The MCAO group received the stroke induction procedure without any drug treatment, and the Solvent group, in addition to MCAO, was administered an intraperitoneal injection of DMSO as a vehicle control (with the same intervals as the ATX groups). Three treatment groups were given intraperitoneal injections of ATX at dosages of 25, 50, or 100 mg/kg. The first dose was administered 30 minutes after the stroke induction, with subsequent doses given every 12 hours for a total of 3 days. All animals were assessed daily using a range of neurobehavioral and functional tests, including the Bederson neurological score, rotarod balance test, shuttle box passive avoidance test, and the Morris water maze memory test. After this testing period, CSF was collected from each rat for cytokine evaluation prior to euthanasia. Brain tissue was then harvested; two brains from each group were designated for qualitative histopathological analysis with H&E staining, and the remaining six were used to quantify cerebral edema percentage.

All the injections were administered intraperitoneally (IP) 30 minutes after stroke induction and were repeated every 12 hours for up to 3 days (6 total doses after MCAO induction).

#### Inclusion Criteria

 Animals demonstrating neurological deficits in pre-tests that were indicative of a successful MCAO procedure (in groups induced by stroke).

#### Exclusion Criteria

- Subjects that failed the initial pre-test assessments.
- Those that did not develop observable neurological deficits following stroke induction, suggesting an unsuccessful MCAO.
- Animals experiencing major non-neurologic post-surgical sequel, such as infection or bleeding, which could compromise their well-being and skew experimental outcomes.
- Any subject that died prior to the scheduled conclusion of the study.
- Low motivation for the dark room in the shuttle box test (step-through latency duration exceeds 60 seconds)

#### MCAO Induction Model

Focal cerebral ischemia was induced using the transient intraluminal filament middle cerebral artery occlusion (tifMCAO) model, as previously described (Mahyar et al., 2025; Themistoklis et al., 2022). Briefly, Wistar rats (weighing 300–400 g) were anesthetized with isoflurane and positioned supine on a heating pad to maintain body temperature at ~37°C. A midline or right paramedian neck incision (~2–3 cm) was made. The common carotid artery (CCA), external carotid artery (ECA), and internal carotid artery (ICA) were carefully exposed through microsurgical dissection. The superior thyroid artery (STA) and occipital artery were coagulated and divided. A complete arteriotomy of the ECA stump was performed. Temporary clips were placed on the CCA and ICA, and a silicone-coated nylon monofilament (diameter ~0.28–0.38 mm) was introduced through the ECA stump and advanced intracranially along the ICA approximately 18–20 mm until resistance was felt, indicating occlusion of the middle cerebral artery origin. After 60 minutes of occlusion, the filament was withdrawn to allow reperfusion. The ECA stump was

permanently ligated, the wound was closed in layers, and the animals were allowed to recover with postoperative monitoring and analgesia.

#### Neurological Function Assessment

Neurological function was assessed daily for three days according to the Bederson scale (Bieber et al., 2019), graded from 0 to 5 as follows: 0 indicated no deficit; 1 represented forelimb flexion; 2 denoted forelimb flexion combined with reduced resistance when pushed laterally; 3 was assigned for circling to one side; 4 indicated circling accompanied by a depressed level of consciousness; and a score of 5 was given for death or a state of unresponsiveness and immobility.

#### Motor Coordination and Balance Assessment

To evaluate motor coordination and balance in the rats, a rotarod apparatus (Model 6700 MT, Borjsanat Company, IR) was employed each day following MCAO induction. The equipment consists of a rotating rod capable of speeds from 0 to 40 rpm. Prior to testing, the animals were acclimated to the device by being placed on the rod rotating at 10 rpm with an acceleration rate of 7 rpm<sup>2</sup>. One hour after the administration of ATX, the animals were placed on the rotarod, and the latency to fall was recorded, with a maximum cutoff time set at 300 seconds.

# Spatial Learning, Memory, and Visual-Motor Abilities

Spatial learning and memory capabilities were evaluated daily after MCAO induction using the morris water maze (MWM) (Nunez, 2008; Othman et al., 2022). The apparatus consisted of a circular water tank (140 cm in diameter, 55 cm high) filled with water ( $20 \pm 1^{\circ}$ C) to a depth of 25 cm and divided in four imaginary quadrants. A submerged platform (11 cm in diameter), hidden 1 cm beneath the water's surface, was positioned in the center of one quadrant (the target quadrant). All trials were video-recorded and analyzed with EthoVision XT 10.1 software (Noldus Information Technology, Netherlands) to quantify swimming velocity and the time percentage

spent in the target quadrant. Twenty-four hours prior to formal training, rats were allowed a 1-minute habituation period in the pool without the platform. The training phase spanned two consecutive days, with four trials per day. During these trials, the platform remained stationary in its designated quadrant. For each trial, a rat was released from one of four randomized start locations (north, south, east, or west) facing the wall. The trial concluded when the animal located the platform or after a 60-second cutoff. A 50-second inter-trial rest period was provided, comprising 20 seconds on the platform and 30 seconds in a dry cage. Animals that failed to find the platform within the time limit were gently guided to it. Following the trials, the rats were dried and returned to their home cages. A probe test (recall test) was administered 24 hours after the final training session. The platform was removed, and each rat was released from a novel starting point. Their behavior was tracked for 60 seconds to measure the duration spent in the target quadrant. Fifteen minutes later, a visible platform test was conducted, where the platform, marked with aluminum foil, was placed in a different quadrant. This test was used to control for potential effects of the treatment on visual-motor function and motivation.

## Passive Avoidance Learning Assessment

The passive avoidance learning (PAL) test was conducted daily after the MCAO induction using a shuttle box apparatus and the mean of results were compared between groups. The shuttle box apparatus was constructed from plexiglass, divided into two equal-sized compartments ( $20 \times 40 \times 20$  cm). These sections differed in illumination: one was brightly illuminated by a 100-watt overhead lamp, and the other was kept dark. The compartments were separated by a guillotine door measuring  $5.7 \times 5.7$  cm. Both sections featured a floor made of 2-mm stainless steel rods spaced 1 cm apart. The floor in the dark compartment was wired to an electrical stimulator to

administer a predefined foot shock to the subjects. The PAL test was conducted following a threephase protocol:

- a) Acclimatization: To habituate the animal to the apparatus, it was placed in an illuminated compartment. After 10 seconds, the guillotine door was raised. The door was closed once the animal's hind legs fully entered the dark compartment. Following a 30-second interval in the dark, the animal was returned to its home cage. This procedure was repeated after a 30-minute delay. The step-through latency (STL), defined as the time taken to move from the light to the dark chamber during this phase, was recorded. Animals exhibiting an STL greater than 60 seconds were excluded from the study due to insufficient innate preference for the dark environment.
- b) Training (Acquisition): The training trial commenced 30 minutes after the second acclimatization. The animal was again placed in the light chamber. After 10 seconds, the door was opened. Upon entry into the dark section, the door was closed and a foot shock (1 Ampere, 50 Hz, and 1.5 s duration) was delivered. The animal was removed after 20 seconds. Two minutes later, it was returned to the light chamber for a retention test; a successful passive avoidance learning outcome was defined as refusing to enter the dark compartment within 120 seconds after the door was opened. If the animal re-entered, the door was closed and the shock was repeated. The number of such training trials required was recorded for each subject.
- c) Recall Test: Memory retention was evaluated 24 hours post-training. The animal was positioned in the light compartment, and the door was opened after a 10-second delay. During a 300-second observation period, the STL, the total time spent in the illuminated compartment, and the number of entries into the dark chamber were documented. For the statistical analysis in this investigation, the STL and the time spent in the light compartment were the primary measures utilized.

These measurements evaluate learning and memory retention by quantifying the animal's success in remembering and evading the context where an aversive foot shock was administered.

## Measurement of Cytokines in the Cerebrospinal Fluid (CSF)

At the end of the three day duration of behavioral tests, rats were first anesthetized using ketamine (50 mg/kg) and xylazine (10 mg/kg), then secured in a stereotaxic apparatus after shaving the posterior neck area. With the head angled at 45 degrees, a 200  $\mu$ L sample of CSF was withdrawn from the cisterna magna using a Hamilton syringe and polyethylene tubing, with its exact coordinations described in reference (Shimizu et al., 2022). To prevent hemo-contamination, the fluid was aspirated carefully. The collected CSF was immediately placed in an Eppendorf tube and flash-frozen in liquid nitrogen. Subsequently, the concentrations of interleukin-10 (IL-10) and interleukin-1 $\beta$  (IL-1 $\beta$ ) in these samples were determined using commercially available rat-specific ELISA kits (MyBiosource, Inc., San Diego, CA, USA; MBS2020828 [detection range of 7.8-500 pg/mL and sensitivity of < 3.5 pg/mL] and MBS2023030 [detection range of 15.6-1000 pg/mL and sensitivity of < 5.4 pg/mL]), following the protocols provided by the manufacturer.

## Qualitative Histopathological Assessments

After CSF collection, two rats in each group were randomly selection for qualitative histopathological assessments. For histopathological analysis, brain tissue was collected from each experimental group following euthanasia. Euthanasia was induced using an intraperitoneal injection of sodium thiopental (20 mg per 100 g of body weight, from a 60 mg/ml solution). Subsequently, the rats underwent transcardial perfusion, first with 0.9% saline and then with a 4% paraformaldehyde solution. The brains were then extracted and post-fixed by immersion in 10% buffered formalin for 48 hours at room temperature. After fixation, the tissue samples were dehydrated through a graded ethanol series, cleared in xylenol, and finally embedded in paraffin

blocks. Using a microtome, sequential 5-µm thick coronal sections were prepared and stained with hematoxylin and eosin (H&E) for examination. The analysis focused primarily on the CA1 area of the hippocampus. Hippocampal sections were specifically obtained from the dorsal hippocampus at the stereotaxic coordinates -4.56 mm from Bregma, with a depth and laterality of 3.5 mm.

#### **Cerebral Edema Assessment**

The calculation of brain edema was performed on the remaining six rats in each group using a formula derived from prior research (Rahimi et al., 2021):

Cerebral edema percentage (brain water content) = 
$$\frac{\textit{wet brain weight-dry brain weight}}{\textit{wet brain weight}} \times 100$$

#### **Statistics**

Statistical analyses were conducted using GraphPad Prism 8 software. Quantitative data were assessed for normality of distribution. Provided that assumptions were met, comparisons across groups were performed using repeated-measures ANOVA, followed by one-way ANOVA. When applicable, the Newman-Keuls post hoc test was employed. For all two-sided comparisons, Tukey's post hoc test was applied where appropriate. The results are expressed as the mean  $\pm$  standard error of the mean (SEM). A probability value of P  $\leq$  0.05 was considered statistically significant for all tests.

#### Results

Efficacy of ATX on neurological function, motor and balance function, and spatial memory

The MCAO and DMSO (Solvent) groups demonstrated markedly elevated Bederson scores relative to the Intact and Sham groups (P < 0.001). Administration of low and medium doses of

ATX resulted in a significant reduction of these neurological deficit scores compared to the MCAO and Solvent groups (P < 0.001 and P < 0.01, respectively). In contrast, the high-dose QC group showed no statistically significant improvement (Figure 2 A).

A similar pattern was observed in the rota-rod test, where the latency to fall was significantly longer in the low and medium-dose ATX groups compared to the untreated MCAO and DMSO controls (P < 0.001 and P < 0.01, respectively). Again, the high-dose group performance did not differ significantly (Figure 2 B).

Regarding rats performance on the shuttle box test, no significant differences were observed in the number of acquisition trials across the experimental groups (Figure 2 C). The analysis indicated that animals receiving low and medium ATX doses demonstrated a statistically significant enhancement in both the duration spent in the dark compartment (Figure 2 D) and STL (Figure 2 E). Conversely, the high-dose treatment group failed to exhibit any significant improvements in these metrics relative to controls.

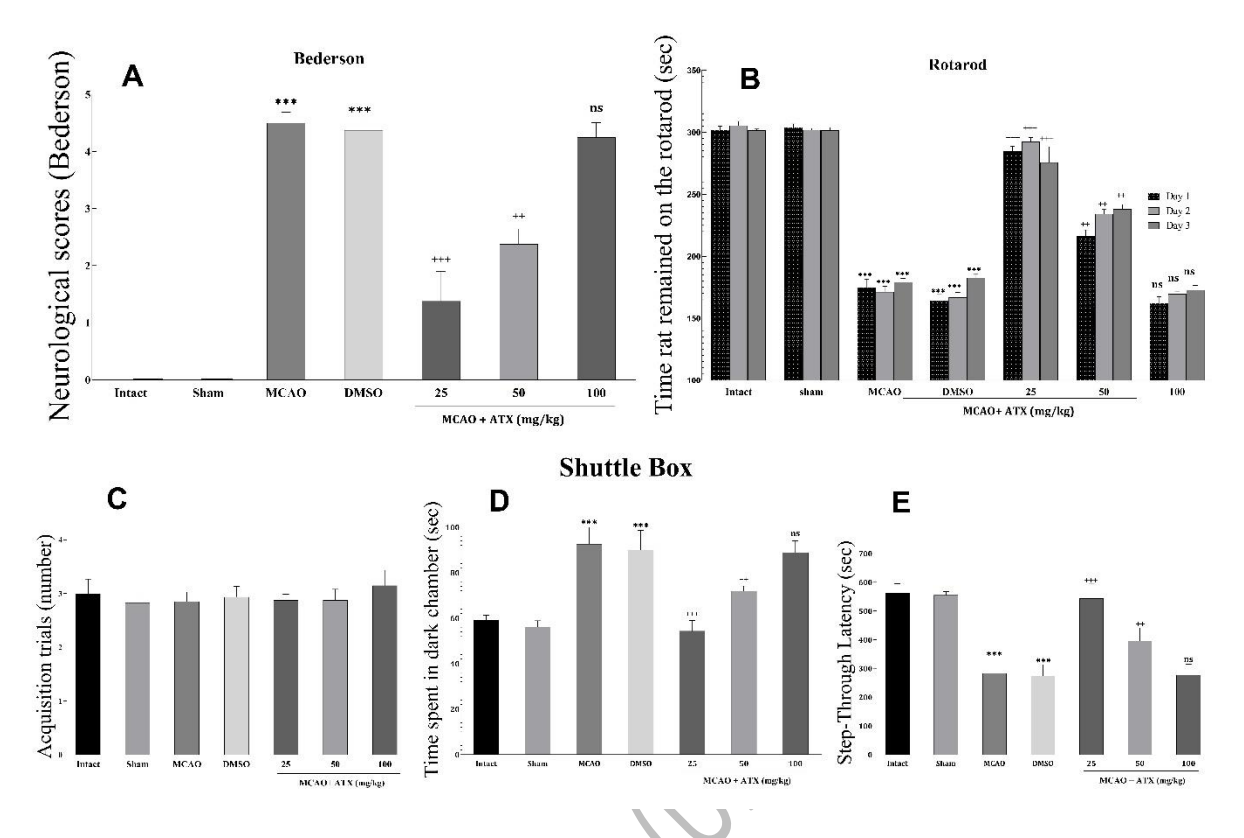


**Figure 2.** Results of neurobehavioral and functional tests. A: Bederson neurologic scores; B: The time rats were able to remain and keep balance on the Rota-Rod device; C, D, and E: Shuttle box spatial memory test results; C: The number of trials required for learning in the shuttle box; D: The time spent in the dark chamber; E: The time duration rats stayed in the light chamber before entering the dark room (step-through). (\*\*\* P < 0.001, P < 0.001,

# Efficacy of ATX on Spatial Learning Results in the MWM test

In the MWM, rats treated with low and medium concentrations of ATX exhibited significantly better spatial learning and memory than the MCAO and DMSO (Solvent) groups. This was evidenced by shorter latencies to find the hidden platform (Figure 3 A), a shorter total path length to the platform (Figure 3 B), more time spent in the target quadrant (Figure 3 C), and a higher frequency of entries into the correct quadrant (Figure 3D). No significant cognitive enhancement was detected in the high-dose group.

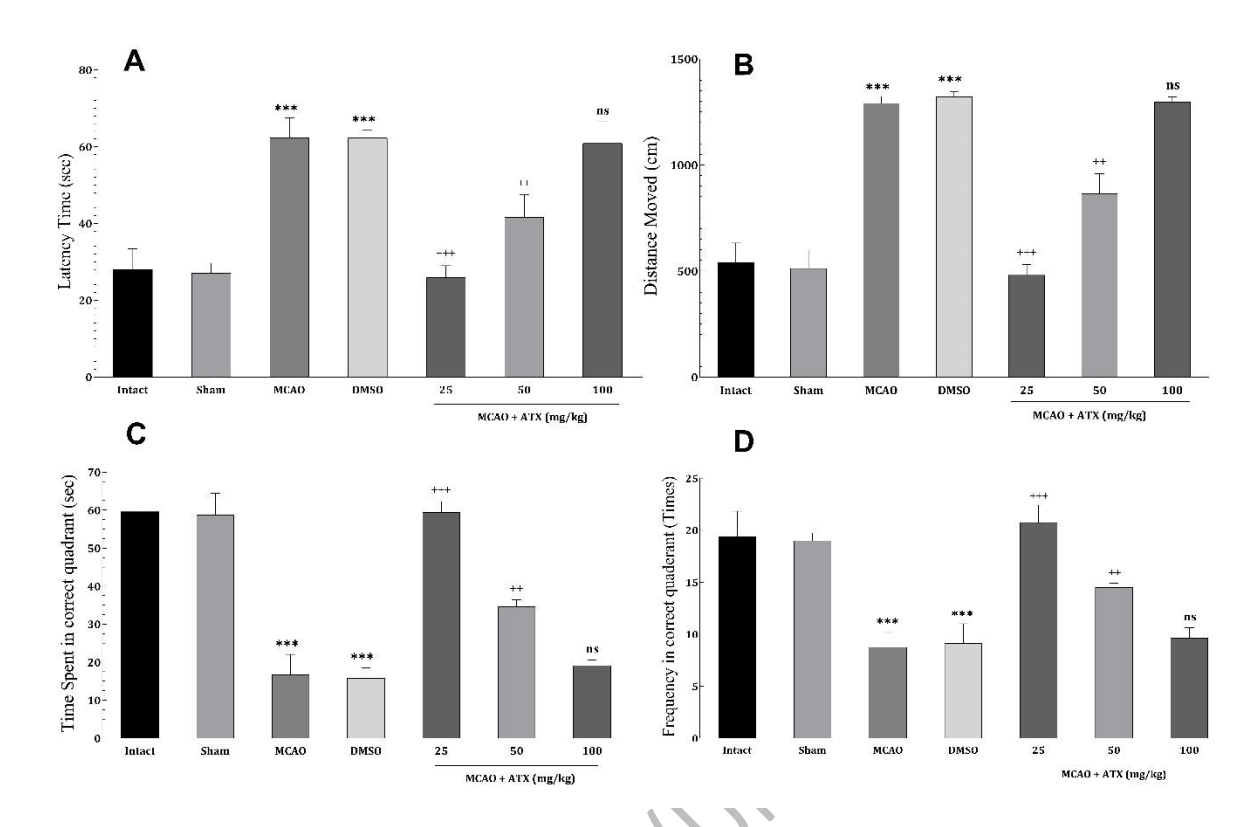


**Figure 3.** MWM test results. A: The time taken by the rats to reach the hidden platform; B: The distance traveled to reach the hidden platform; C: The total time duration rats spent in the correct quadrant; D: The number of times rats were present in the correct quadrant. (\*\*\* P < 0.001, + P < 0.05, ++ P < 0.01, +++ P < 0.001, ns: not significant).

### Efficacy of ATX on Interleukin Levels

The analysis of cytokine levels showed that the low- and medium-dose groups exhibited a significantly elevated IL-10 concentration alongside a markedly reduced IL-1 $\beta$  level compared to the MCAO and DMSO (Solvent) control groups. In contrast, no significant alterations in either interleukin were detected in the high-dose group.

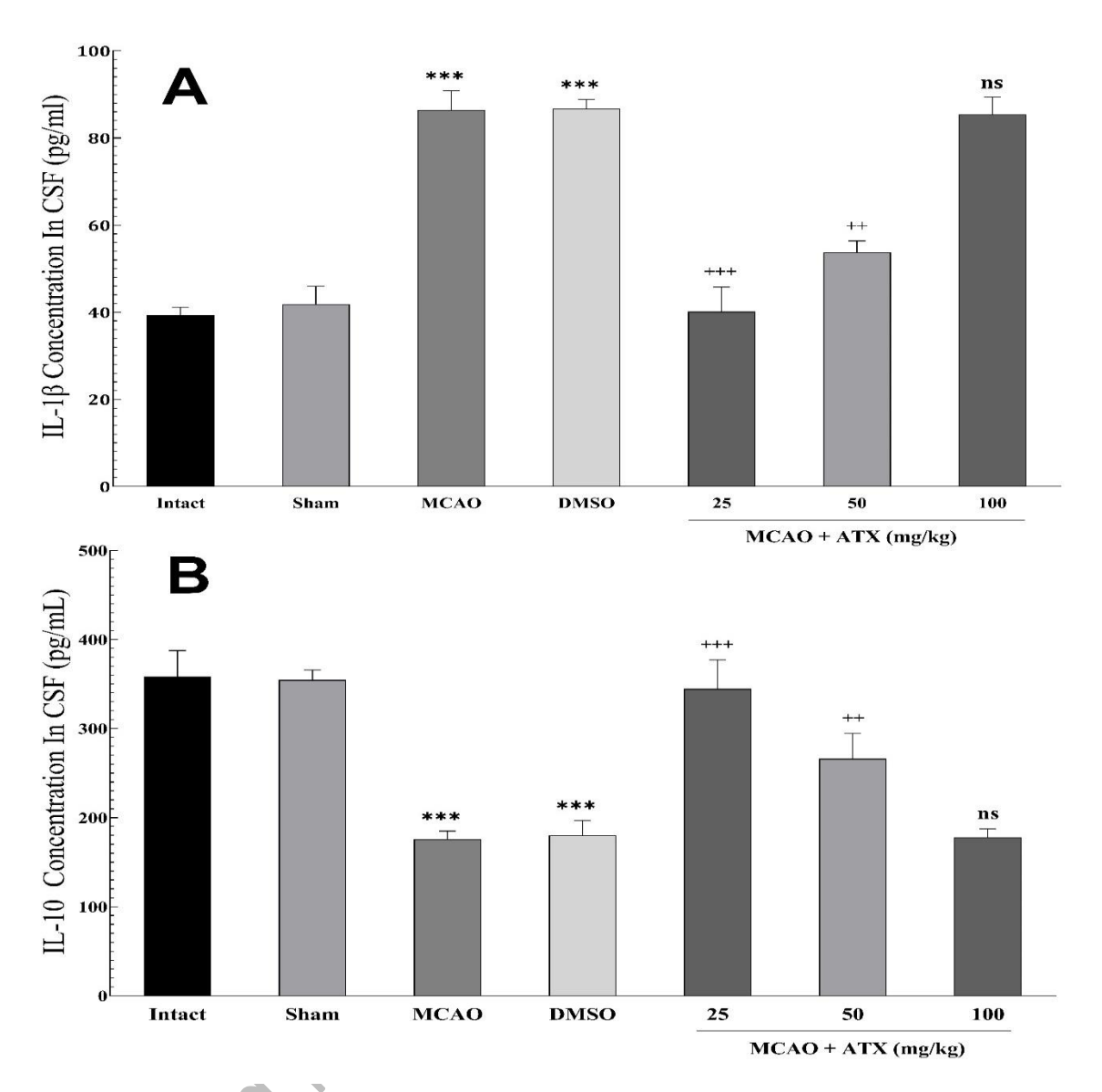


**Figure 4.** Concentration of interleukins in the CSF. A: Concentration of IL-1 $\beta$  in the CSF; B: Concentration of IL-10 in the CSF (\*\*\* P < 0.001, +P < 0.05, ++ P < 0.01, +++ P < 0.001, ns: not significant).

#### Efficacy of ATX on Cerebral Edema

Cerebral edema, measured by brain water content (BWC), was markedly elevated in the MCAO and DMSO (Solvent) groups compared to the Intact and Sham controls (P < 0.001), confirming a rise in edema following stroke induction. Treatment with low and medium doses of ATX produced a significant reduction in BWC (P < 0.001 and P < 0.01, respectively). The low dosage demonstrated the most potent effect in mitigating this edema. Conversely, the group administered the high dose of ATX showed no statistically significant difference from the stroke control groups (Figure 5).

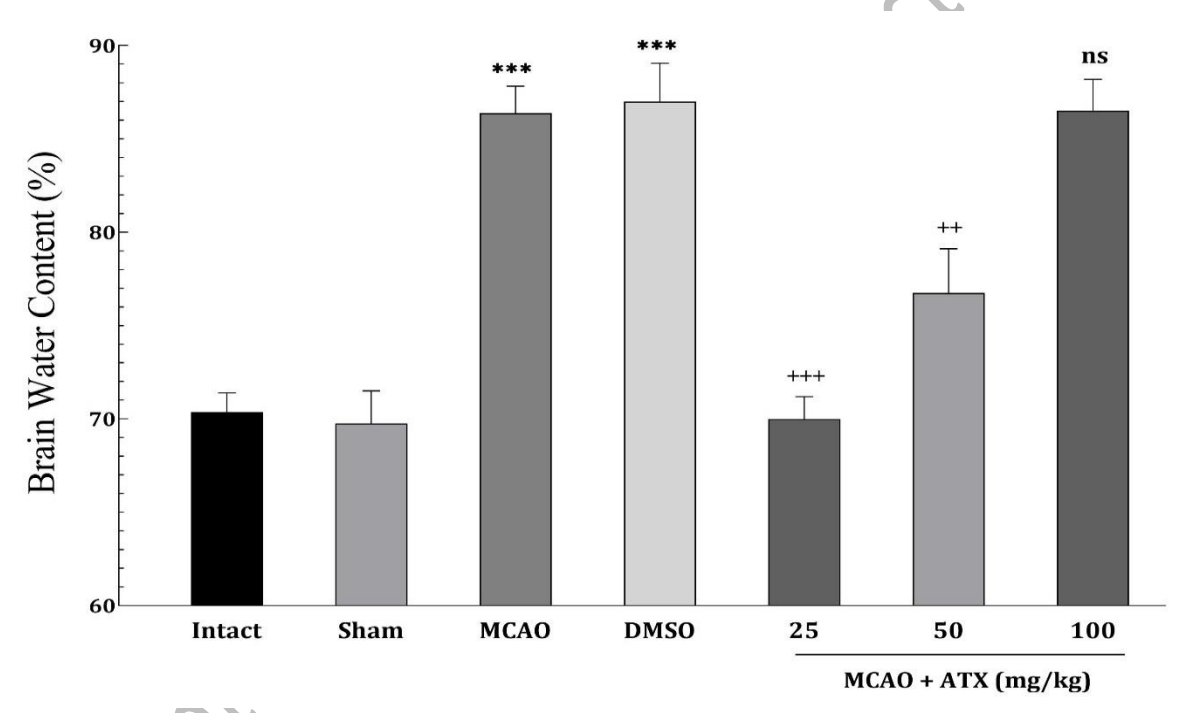


**Figure 5.** Cerebral edema presented as percentage of water in brain (\*\*\* P < 0.001, + P < 0.05, ++ P < 0.01, +++ P < 0.001, ns: not significant).

# Qualitative Histopathological Assessments of ATX Neuroprotective Effects on Hippocampal CA1 Region

As shown in Figure 6, the control groups without induced stroke (A, B) show normal neuronal cytoarchitecture, featuring distinct nuclei and no indications of apoptosis. Conversely, the stroke

model groups (C, D) demonstrate extensive cellular damage, including pronounced pyknotic nuclei and condensed chromatin. ATX administration at 25 mg/kg (E) and 50 mg/kg (F) promoted notable neuronal recovery, with a majority of cells displaying near-normal morphology and clear nuclei, despite some residual apoptotic cells. In contrast, the 100 mg/kg ATX (G) dosage did not confer a significant protective effect, as the tissue morphology was comparable to the untreated stroke groups.

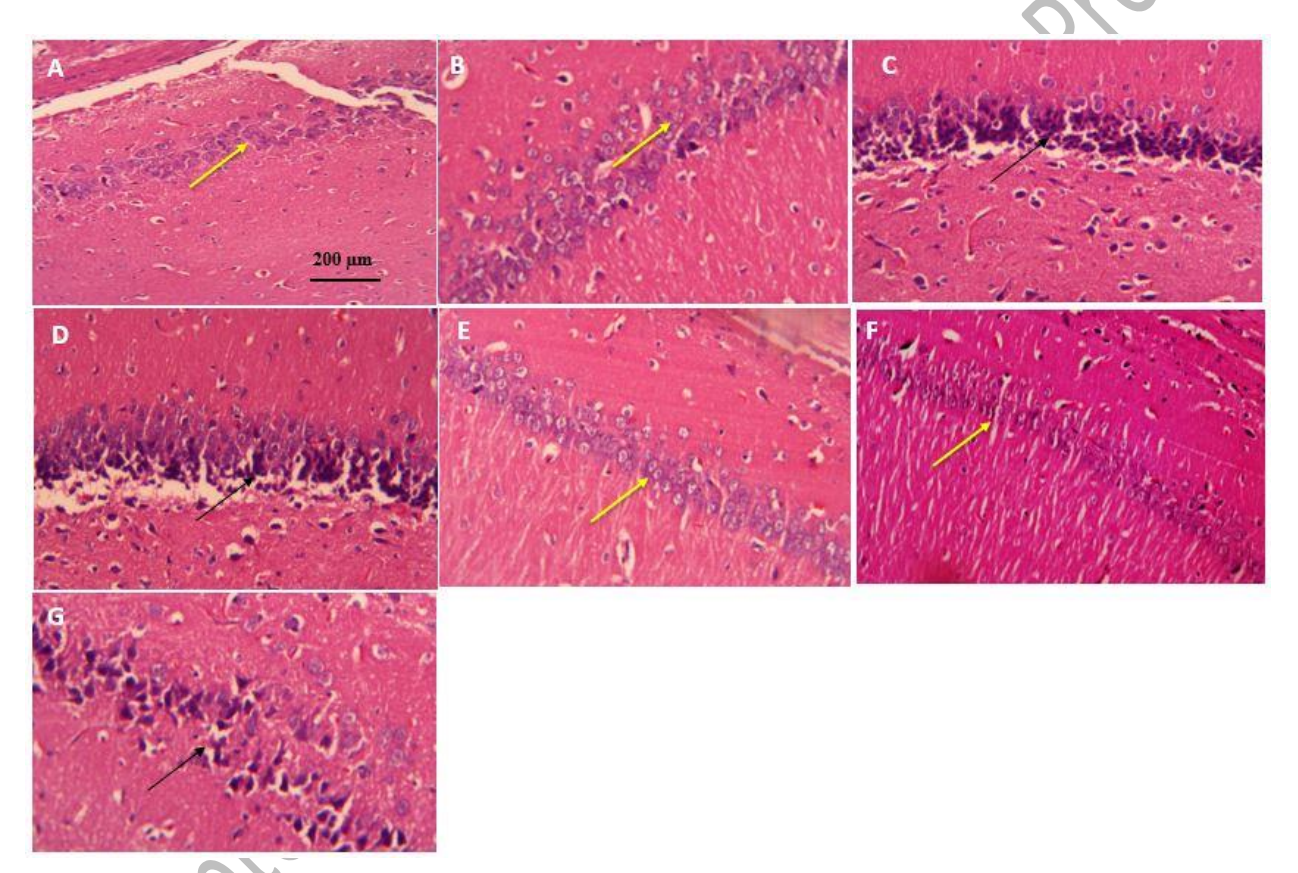


**Figure 6.** Qualitative histopathological assessment of the hippocampal CA1 region using H&E staining and magnification of 200x. (A) Intact; (B) Sham; (C) MCAO; (D) Vehicle; (E) ATX 25 mg/kg; (F) ATX 50 mg/kg; (G) ATX 100 mg/kg; Yellow arrows indicate normal neurons; Black arrows indicate necrotic neurons.

### **Discussion**

This study sought to examine the neuroprotective potential of ATX following MCAO in rats. The results indicate that ATX, at doses of 25 and 50 mg/kg, conferred significant protection, which was evidenced by improved neurobehavioral and functional outcomes, reduced cerebral edema, and enhanced histological preservation (with the lowest dose demonstrating the best improvements). However, these beneficial effects were not observed at the higher dose of 100 mg/kg, suggesting a loss of efficacy.

ATX demonstrates robust neuroprotective effects against cerebral ischemia/reperfusion (I/R) injury, as evidenced by consistent improvements in neurological function, reduced infarct volume, and decreased neuronal loss in various animal models. Its efficacy is observed with both pre- and post-I/R administration, via oral or intraperitoneal routes, across a wide dose range. The protective mechanisms are multifaceted, primarily involving potent antioxidant activity through the upregulation of the Nrf2/HO-1 signaling pathway and key enzymes like SOD and CAT, leading to reduced oxidative stress markers (Park, 2025; Wang & Qi, 2022). ATX upregulates the cellular antioxidant defense system by activating the Nrf2 signaling pathway. This activation, potentially mediated through the PI3K/Akt and ERK pathways which inhibit GSK3β, leads to the transcription of cytoprotective genes like HO-1, bolstering the brain's resistance to oxidative stress (Wang & Qi, 2022; Wang et al., 2024). Recent studies confirm that ATX treatment in cerebral IR models restores. Glutathione (GSH) levels and SOD activity while significantly suppressing the concentration of Malondialdehyde (MDA), a key marker of lipid peroxidation (Galasso et al., 2018).

ATX also exerts strong anti-apoptotic effects by modulating the balance of Bcl-2 and Bax proteins, inhibiting caspase activation, and protecting mitochondrial integrity. A critical neuroprotective

effect of ATX is its ability to counter programmed cell death, including both apoptosis and parthanatos. It achieves this by increasing anti-apoptotic Bcl-2 and decreasing pro-apoptotic Bax, Caspase-3, and Cyt C, while also modulating PARP1 to prevent AIF-mediated parthanatos (Wang et al., 2024). Furthermore, it has been shown to protect neuronal cells from oxidative stress-induced apoptosis by suppressing mitochondrial abnormalities and the creation of intracellular ROS (Galasso et al., 2018).

Furthermore, it suppresses neuroinflammation by reducing pro-inflammatory cytokines such as TNF- $\alpha$  IL-6, or IL-1 $\beta$  (as indicated by the present study), and mitigates excitotoxicity by regulating glutamate levels. This is achieved primarily by suppressing the NF- $\kappa$ B pathway through the inhibition of IKK $\beta$  phosphorylation and the nuclear translocation of the p65 subunit. Additionally, ATX inhibits the MAPK signaling pathways, including p38 and JNK, further curtailing the neuroinflammatory response (Wang & Qi, 2022). Specifically, in activated microglial cells (BV-2 cell line), ATX drastically reduced the release of inflammatory mediators through the modulation of factors involved in the NF- $\kappa$ B cascade (e.g., p-IKK $\alpha$ , p-I $\kappa$ B $\alpha$ , and p-NF- $\kappa$ B p65) and MAPK pathways (Galasso et al., 2018).

Also, ATX modulates neuroinflammation by maintaining the integrity of the BBB, reducing brain edema and preventing the infiltration of peripheral inflammatory cells into the CNS. ATX protects the BBB also by downregulating the astrocytic p75NTR receptor, which leads to increased expression of tight junction proteins ZO-1 and claudin-5, thereby preserving BBB integrity and reducing the risk of hemorrhagic transformation (Wang et al., 2024). It also exhibits systemic anti-inflammatory properties, alleviating peripheral inflammation which can exacerbate neuroinflammation (Wang & Qi, 2022).

Additionally, ATX promotes neural regeneration and functional recovery by activating the cAMP/PKA/CREB pathway and increasing expression of growth factors like BDNF and GAP-43. Pre-treatment with ATX has been shown to promote nerve cell regeneration by increasing gene expression of GFAP (important for BBB function and repair), MAP-2 (for microtubule growth and neuronal regeneration), BDNF, and GAP-43. It also promotes neurogenesis and improves behavioral performance in hippocampal-dependent tasks, which is a predominant mechanism for countering cognitive decline (Galasso et al., 2018). It also enhances DNA repair by reducing the DNA damage marker 8-OHdG and increasing the expression of the DNA repair protein PARP1 (116kDa), as well as upregulating NQO1 and Hsp70, which collectively help maintain genomic integrity and promote cell survival (Wang et al., 2024). A key feature enabling these neurological activities is its lipid-soluble nature, which allows it to cross the BBB and accumulate in brain regions such as the hippocampus and cerebral cortex (Si & Zhu, 2022). It is important to note that natural ATX (from sources like Haematococcus pluvialis) is esterified, which confers higher bioavailability compared to the synthetic, unesterified version, making the natural form significantly superior in its antioxidant and anti-inflammatory properties (Galasso et al., 2018). Similar to our study, Taheri et al. (Taheri et al., 2022) investigated the dose-dependent effects of on I/R-induced brain injury in a rat MCAO model. ATX administration, particularly at the medium dose of 45 mg/kg, significantly reduced stroke volume and improved neurological sensorimotor deficits. Mechanistically, ATX demonstrated potent antioxidant properties by reducing lipid peroxidation (MDA) and restoring the total oxidant status (TOS) and glutathione (GSH) levels towards normal. It enhanced the activity of the antioxidant enzyme glutathione peroxidase (GPX) and increased the gene expression of key antioxidant enzymes, including catalase, SOD, and GPX, which were suppressed after ischemia. A significant and novel finding was ATX's pronounced

upregulation of the glutamate transporter GLT-1 (EAAT2), which is crucial for clearing excess synaptic glutamate and preventing excitotoxicity. The study concluded that the 45 mg/kg dose was most effective for the primary endpoints of stroke volume and neurological function, highlighting that the timing of administration (acutely after occlusion and before reperfusion).

Both studies found a clear relationship between ATX administration and consequent improved outcomes (function, edema, anti-inflammation). These effects were seen in Taheri et al.'s study with a single acute dose administration while we studied a repeated-dosing protocol (Taheri et al., 2022). This is a critical difference. The ineffectiveness of our 100 mg/kg dose, compared to the partial efficacy of Taheri's 65 mg/kg dose, could strongly suggest that dosing frequency and total cumulative exposure are crucial. Our regimen resulted in a much higher total ATX exposure (6 doses of 100 mg/kg vs. 1 dose of 65 mg/kg). It is plausible that very high, repeated doses may lead to receptor saturation, feedback inhibition, or even pro-oxidant effects, explaining the loss of efficacy we observed. This highlights a path towards which future studies can be formed.

Xue et al. (Xue et al., 2017) demonstrated that ATX treatment ameliorated learning and memory deficits in a mouse model of vascular cognitive impairment induced by repeated cerebral ischemia/reperfusion. The study found that ATX administration rescued the loss of pyramidal neurons in the hippocampal CA1 and CA3 regions. Mechanistically, ATX decreased oxidative stress, as evidenced by a reduction in malondialdehyde (MDA) and increases in the antioxidants GSH and SOD. Furthermore, ATX reduced ultrastructural damage to neurons and mitochondria observed via electron microscopy. The anti-apoptotic effect of ATX was confirmed through the modulation of key proteins; it decreased the expression of pro-apoptotic Cytochrome C, cleaved Caspase-3, and Bax, while increasing the expression of the anti-apoptotic protein Bcl-2. The study

concluded that ATX protects against cognitive deficits and neuronal damage primarily by attenuating oxidative stress and subsequent apoptosis.

We used a focal ischemia model (transient MCAO), which mimics a localized stroke, such as an embolic clot in a major cerebral artery; but Xue et al. (Xue et al., 2017) used a global ischemia model (repeated BCCAO), which induces widespread cerebral hypoperfusion and is a model for vascular cognitive impairment. We employed a repeated-dosing protocol (IP injection every 12 hours for 3 days, 6 total doses) across a range of doses (25, 50, 100 mg/kg); however, Xue et al. (Xue et al., 2017) used a single, lower dose (10 mg/kg) administered daily via intragastric gavage for a much longer duration (28 days). This is a critical difference. Our study's investigation of multiple doses and the discovery of an inverted dose-response curve is a significant advancement and identifies a potential therapeutic window for ATX, which was not explored in the Xue et al. (Xue et al., 2017) study.

The study by Park et al. (Park et al., 2022) investigated the neuroprotective effects of ATX against severe I/R injury in the forebrain of gerbils. The model used was a 15-minute transient bilateral common carotid artery occlusion, which induces massive, delayed neuronal death across the hippocampal CA1-3 regions. The research employed a pre-treatment protocol, administering a high dose of ATX (100 mg/kg, intraperitoneally) once daily for three consecutive days prior to the induction of ischemia. The key findings were that ATX pre-treatment significantly attenuated the severe I/R-induced loss of pyramidal neurons in the hippocampal CA1-3 areas, as confirmed by Nissl staining, NeuN immunohistochemistry, and reduced Fluoro-Jade B staining (a marker for neuronal degeneration). The proposed mechanism for this neuroprotection was a potent reduction in oxidative stress. This was evidenced by ATX's ability to significantly decrease immunoreactivity for markers of oxidative DNA damage (80HdG) and lipid peroxidation (4HNE)

in the hippocampal neurons one day after I/R. Furthermore, ATX pre-treatment itself boosted the baseline levels of the key antioxidant enzymes SOD1 and SOD2 in the hippocampus and helped maintain their expression after I/R, which was otherwise significantly reduced in the untreated I/R group. The study concluded that ATX confers neuroprotection against severe ischemic brain injury primarily through its robust antioxidant activity, which mitigates oxidative damage to cellular components.

Our study used a focal ischemia model in rats (transient MCAO) which mimics a localized stroke, such as an embolic clot blocking a major cerebral artery; however, Park et al. (Park et al., 2022) used a global forebrain ischemia model in gerbils (15-minute bilateral CCA occlusion) which mimics conditions like cardiac arrest, leading to widespread hippocampal damage. Our rat MCAO model is more clinically relevant for the most common type of human stroke. Additionally, we employed a post-treatment, repeated-dosing protocol (25, 50, 100 mg/kg, IP, 30 mins after MCAO and every 12 hours for 3 days). The most significant finding was an inverted dose-response, where 25 and 50 mg/kg were effective, but 100 mg/kg lost all efficacy; however, Park et al. (Park et al., 2022) employed a pre-treatment protocol with a high dose regimen (100 mg/kg, IP, once daily for 3 days before ischemia) which was highly effective in providing neuroprotection. This is the most critical difference. The core of the discrepancy lies not in the dose itself, but in the interaction between the dose, the dosing regimen, and the pathological context. Administering ATX before the ischemic insult acts as a pharmacological preconditioning agent; thus, when the severe ischemia hit, the brain was already in a heightened state of defense, allowing it to better withstand the oxidative burst upon reperfusion (such as in the Park et al study). On the other hand, in a posttreatment approach, the injury cascade (excitotoxicity, oxidative stress, inflammation) was already initiated by the time the first dose was given 30 minutes post-MCAO (such as in our study). In this

context, a single high dose might be beneficial, but repeated high doses (6 injections of 100 mg/kg) in an already compromised brain may overwhelm or disrupt the very pathways you are trying to activate. Future studies should be designed to directly test this hypothesis. Future studies can conduct a study with identical high (100 mg/kg) and medium (50 mg/kg) doses of ATX, but administer them in different temporal regimens: pre-ischemia only, post-ischemia only (as in your study), and a combination of both. Compare outcomes to pinpoint the critical window and interaction with injury progression.

The research by Lu et al. (Lu et al., 2010) demonstrates that ATX pretreatment provides significant neuroprotection against cerebral I/R injury. In their in vivo rat MCAO model, intragastric administration of ATX (50 and 80 mg/kg) prior to ischemia dramatically reduced infarct volume and improved neurological scores in a dose-dependent manner, with 80 mg/kg being the most effective. Histological analysis via Nissl staining confirmed that ATX reduced neuronal loss. The proposed mechanism is primarily rooted in its potent antioxidant activity. Their in vitro experiments showed that ATX attenuated H<sub>2</sub>O<sub>2</sub>-induced cytotoxicity and apoptosis in cortical neurons and restored the mitochondrial membrane potential, suggesting the mitochondrial pathway is key to its protective effect. The study concludes that ATX's free radical scavenging activity and its ability to enhance membrane stability are central to its neuroprotective properties. In another study by Yegin et al. (Yeğin et al., 2023) further supports the neuroprotective and antioxidant role of ATX in a cerebral ischemia-reperfusion model. They found that pre-ischemic IP administration of ATX (25 and 75 mg/kg) significantly mitigated oxidative stress. This was evidenced by a dose-dependent increase in the activity of antioxidant enzymes SOD and CAT and a decrease in the lipid peroxidation marker MDA, with the high dose (75 mg/kg) showing the strongest effect, even bringing MDA below control levels. Histologically, both ATX doses reduced

neuronal necrosis and damage in the cerebral cortex compared to the sham group, indicating a tangible neuroprotective effect.

Out study revealed a clear inverted dose-response curve. The low (25 mg/kg) and medium (50 mg/kg) doses were highly effective, while the high dose (100 mg/kg) showed no significant benefit across all parameters. However, Lu et al. (Lu et al., 2010) and Yegin et al. (Yeğin et al., 2023) both reported a linear or positive dose-response within their tested ranges, where a higher dose conferred greater protection. This is the most critical difference and is likely due to the dosing regimen. Our study used a post-treatment, repeated-dosing protocol (6 doses over 3 days), resulting in a much higher cumulative exposure (600 mg/kg total for the high-dose group). In contrast, Lu et al. and Yegin et al. used a single, pre-ischemic dose.

Similarly, Pan et al. (Pan et al., 2017) used a preventive, pre-treatment protocol (oral administration for 7 days before MCAO). They reported a linear or positive dose-response, with a higher dose (10 mg/kg) being more effective than a lower one (5 mg/kg). Shen et al. (Shen et al., 2009) used a single, acute pre-treatment dose administered directly into the brain (interacerebroventricular) just before MCAO. While the stroke models are similar, the route of administration differs between studies. Ours IP and Pan's oral routes are more clinically translatable than the ICV route used by Shen et al (Shen et al., 2009). Nevertheless, the consistency of effects across oral, IP, and ICV routes strengthens the evidence for ATX's efficacy, provided the dosing regimen is appropriate.

Future research must systematically investigate the therapeutic window for ATX administration, determining the optimal time post-stroke for intervention. Furthermore, studies should explore the effects of chronic, lower-dose administration to align with practical clinical scenarios for secondary prevention or recovery. The stark difference in efficacy between pre-treatment and our

post-treatment, repeated-dosing regimen highlights the necessity of understanding the pharmacodynamics of ATX in the dynamically changing post-ischemic brain environment. To robustly bridge the gap between these promising preclinical results and human trials, future work should adhere to established translational guidelines, such as the STAIR (Stroke Therapy Academic Industry Roundtable) recommendations, including but not limited to:

- Confirming efficacy in higher-order species (e.g., non-human primates) with more humanlike brain anatomy.
- Assessing recovery over weeks or months to ensure sustained benefit and functional relevance.
- Investigating ATX in conjunction with existing recanalization therapies (like tPA or thrombectomy) to model real-world clinical use and assess for synergistic effects.
- Developing clinically viable formulations (e.g., for intravenous administration in acute settings) and conducting detailed pharmacokinetic and toxicological studies to define safe dosing parameters in humans.

# **Conclusion**

In conclusion, this study demonstrates that ATX, administered post-ischemia, confers significant neuroprotection in a rat focal transient MCAO model. The treatment with 25 and 50 mg/kg doses effectively improved neurological and cognitive function, reduced cerebral edema, modulated the neuroinflammatory response by increasing IL-10 and decreasing IL-1β, and preserved the histological integrity of the vulnerable hippocampal CA1 neurons, with the lower 25 mg/kg dose demonstrating the most beneficial effects. The most salient finding; however, is the loss of therapeutic efficacy at the higher dose of 100 mg/kg, revealing a distinct inverted dose-response

relationship. This underscores that the neuroprotective benefits of ATX are critically dependent on dosing regimen and timing relative to the ischemic insult. These findings position ATX as a promising candidate for stroke therapy but necessitate careful, systematic future investigation to delineate its optimal clinical application window and dosage to harness its full therapeutic potential while avoiding the loss of effect at higher exposures.

#### **Statements and Declarations**

Ethics approval and consent to participate: This study was conducted without commercial input or involvement in the design, implementation, analysis, or reporting. This study was approved by the Research Ethics Committee of Laboratory Animals, Mazandaran University of Medical Sciences (Ethics Approval Code: IR.MAZUMS.AEC.1403.031). All procedures performed in this study were in accordance with the ARRIVE guidelines and the ethical standards of the Institutional Research Ethics Committee of Mazandaran University of Medical Sciences and in accordance with the Guidance on the Operation of the Animals (Scientific Procedures) Act 1986 and associated guidelines.

Consent for publication: Not applicable.

**Availability of data and materials:** The data are available upon reasonable request from the corresponding author.

**Competing interests:** The authors declare that they have no conflicts of interest related to this study.

**Funding:** Partial financial support for this project was provided by the Mazandaran University of Medical Sciences (18994).

**Author contributions** (author initials): Conceptualization: ASK and EG; Data curation: PP, MG, and MP; Formal analysis: ASK and SBK; Methodology: ASK; Project administration: ASK, PP, MG, and MP; Resources: ASK; Software: ASK, EG, and SBK; Supervision: ASK; Validation: EG and SBK; Visualization: EG, MG, and SBK; Writing—original draft: MG, EG, and SBK; Writing—review & editing: All authors.

chnology of Ma

chnology of Ma Acknowledgments: We thank the Deputy of Research and Technology of Mazandaran University

## References

- Ashrafizadeh, M., Ahmadi, Z., Yaribeygi, H., Sathyapalan, T., & Sahebkar, A. (2022). Astaxanthin and Nrf2 signaling pathway: A novel target for new therapeutic approaches. *Mini Reviews in Medicinal Chemistry*, 22(2), 312-321.
- Bieber, M., Gronewold, J., Scharf, A.-C., Schuhmann, M. K., Langhauser, F., Hopp, S., Mencl, S., Geuss, E., Leinweber, J., & Guthmann, J. (2019). Validity and reliability of neurological scores in mice exposed to middle cerebral artery occlusion. *Stroke*, *50*(10), 2875-2882.
- Brendler, T., & Williamson, E. M. (2019). Astaxanthin: How much is too much? A safety review. *Phytotherapy Research*, 33(12), 3090-3111.
- Galasso, C., Orefice, I., Pellone, P., Cirino, P., Miele, R., Ianora, A., Brunet, C., & Sansone, C. (2018). On the neuroprotective role of astaxanthin: new perspectives? *Marine drugs*, *16*(8), 247.
- Grimmig, B., Kim, S.-H., Nash, K., Bickford, P. C., & Douglas Shytle, R. (2017). Neuroprotective mechanisms of astaxanthin: a potential therapeutic role in preserving cognitive function in age and neurodegeneration. *Geroscience*, *39*(1), 19-32.
- Jurcau, A., & Ardelean, A. I. (2022). Oxidative stress in ischemia/reperfusion injuries following acute ischemic stroke. *Biomedicines*, *10*(3), 574.
- Li, S., Takahara, T., Fujino, M., Fukuhara, Y., Sugiyama, T., Li, X.-K., & Takahara, S. (2017). Astaxanthin prevents ischemia-reperfusion injury of the steatotic liver in mice. *PLoS One*, *12*(11), e0187810.
- Liang, H., Kurimoto, S., Shima, K. R., Ota, T., Minabe, Y., & Yamashima, T. (2016). Why is hippocampal CA1 especially vulnerable to ischemia.
- Lin, L., Wang, X., & Yu, Z. (2016). Ischemia-reperfusion injury in the brain: mechanisms and potential therapeutic strategies. *Biochemistry & pharmacology: open access*, 5(4), 213.
- Lu, Y.-P., Liu, S.-Y., Sun, H., Wu, X.-M., Li, J.-J., & Zhu, L. (2010). Neuroprotective effect of astaxanthin on H2O2-induced neurotoxicity in vitro and on focal cerebral ischemia in vivo. *Brain Research*, *1360*, 40-48.
- Mahyar, M., Ghadirzadeh, E., Nezhadnaderi, P., Moayedi, Z., Maboud, P., Ebrahimi, A., Siahposht-Khachaki, A., & Karimi, N. (2025). Neuroprotective effects of quercetin on hippocampal CA1 neurons following middle cerebral artery ischemia—reperfusion in male rats: a behavioral, biochemical, and histological study. *BMC neurology*, 25(1), 9.
- Nunez, J. (2008). Morris water maze experiment. *Journal of visualized experiments: JoVE*(19), 897.
- Othman, M. Z., Hassan, Z., & Has, A. T. C. (2022). Morris water maze: a versatile and pertinent tool for assessing spatial learning and memory. *Experimental animals*, 71(3), 264-280.
- Otsuka, T., Shimazawa, M., Inoue, Y., Nakano, Y., Ojino, K., Izawa, H., Tsuruma, K., Ishibashi, T., & Hara, H. (2016). Astaxanthin protects against retinal damage: evidence from in vivo and in vitro retinal ischemia and reperfusion models. *Current eye research*, 41(11), 1465-1472.

- Pan, L., Zhou, Y., Li, X.-f., Wan, Q.-j., & Yu, L.-h. (2017). Preventive treatment of astaxanthin provides neuroprotection through suppression of reactive oxygen species and activation of antioxidant defense pathway after stroke in rats. *Brain research bulletin*, 130, 211-220.
- Park, J. H. (2025). Neuroprotective Bioactive Compounds from Marine Algae and Their By-Products Against Cerebral Ischemia–Reperfusion Injury: A Comprehensive Review. *Applied Sciences*, *15*(19), 10791.
- Park, J. H., Lee, T.-K., Kim, D. W., Ahn, J. H., Lee, C.-H., Kim, J.-D., Shin, M. C., Cho, J. H., Lee, J.-C., & Won, M.-H. (2022). Astaxanthin confers a significant attenuation of hippocampal neuronal loss induced by severe ischemia-reperfusion injury in gerbils by reducing oxidative stress. *Marine drugs*, 20(4), 267.
- Qian, Y., Lu, X., Chen, L., Sun, J., Cao, K., Yu, Q., & Shao, J. (2021). Effect of astaxanthin on neuron damage, inflammatory factors expressions and oxidative stress in mice with subarachnoid hemorrhage. *American Journal of Translational Research*, 13(11), 13043.
- Qiu, X., Fu, K., Zhao, X., Zhang, Y., Yuan, Y., Zhang, S., Gu, X., & Guo, H. (2015). Protective effects of astaxanthin against ischemia/reperfusion induced renal injury in mice. *Journal of translational medicine*, 13(1), 28.
- Rahimi, S., Dadfar, B., Tavakolian, G., Rad, A. A., Shabkahi, A. R., & Siahposht-Khachaki, A. (2021). Morphine attenuates neuroinflammation and blood-brain barrier disruption following traumatic brain injury through the opioidergic system. *Brain research bulletin*, 176, 103-111.
- Saini, V., Guada, L., & Yavagal, D. R. (2021). Global epidemiology of stroke and access to acute ischemic stroke interventions. *Neurology*, *97*(20\_Supplement\_2), S6-S16.
- Shen, H., Kuo, C.-C., Chou, J., Delvolve, A., Jackson, S. N., Post, J., Woods, A. S., Hoffer, B. J., Wang, Y., & Harvey, B. K. (2009). Astaxanthin reduces ischemic brain injury in adult rats. *The FASEB journal*, 23(6), 1958.
- Shimizu, K., Gupta, A., Brastianos, P. K., & Wakimoto, H. (2022). Anatomy-oriented stereotactic approach to cerebrospinal fluid collection in mice. *Brain Research*, 1774, 147706.
- Si, P., & Zhu, C. (2022). Biological and neurological activities of astaxanthin. *Molecular medicine reports*, 26(4), 1-12.
- Sun, M.-S., Jin, H., Sun, X., Huang, S., Zhang, F.-L., Guo, Z.-N., & Yang, Y. (2018). Free radical damage in ischemia-reperfusion injury: an obstacle in acute ischemic stroke after revascularization therapy. *Oxidative medicine and cellular longevity*, 2018(1), 3804979.
- Taheri, F., Sattari, E., Hormozi, M., Ahmadvand, H., Bigdeli, M. R., Kordestani-Moghadam, P., Anbari, K., Milanizadeh, S., & Moghaddasi, M. (2022). Dose-dependent effects of astaxanthin on ischemia/reperfusion induced brain injury in mcao model rat. *Neurochemical Research*, *47*(6), 1736-1750.
- Themistoklis, K. M., Papasilekas, T. I., Melanis, K. S., Boviatsis, K. A., Korfias, S. I., Vekrellis, K., & Sakas, D. E. (2022). transient intraluminal filament middle cerebral artery occlusion stroke model in rats: A step-by-step guide and technical considerations. *World Neurosurgery*, *168*, 43-50.

- Wang, S., & Qi, X. (2022). The putative role of astaxanthin in neuroinflammation modulation: Mechanisms and therapeutic potential. *Frontiers in Pharmacology*, *13*, 916653.
- Wang, X., Li, H., Wang, G., He, Z., Cui, X., Song, F., Li, J., & Zhang, L. (2024). Therapeutic and preventive effects of astaxanthin in ischemic stroke. *Frontiers in Nutrition*, 11, 1441062.
- Xue, Y., Qu, Z., Fu, J., Zhen, J., Wang, W., Cai, Y., & Wang, W. (2017). The protective effect of astaxanthin on learning and memory deficits and oxidative stress in a mouse model of repeated cerebral ischemia/reperfusion. *Brain research bulletin*, 131, 221-228.
- Yang, B.-b., Zou, M., Zhao, L., & Zhang, Y.-K. (2021). Astaxanthin attenuates acute cerebral infarction via Nrf-2/HO-1 pathway in rats. *Current Research in Translational Medicine*, 69(2), 103271.
- Yeğin, B., Öz, S., Dönmez, D. B., Özden, H., Üstüner, M. C., Kabay, S. C., & Yücel, F. (2023). Effect of Dose-Related Astaxanthin on Rats with Cerebral Ischemia-Reperfusion. *Yüksek İhtisas Üniversitesi Sağlık Bilimleri Dergisi*, 4(2), 42-49.
- Yuguang, Y., Changping, L., & Jiajia, H. (2025). Effects of astaxanthin on oxidative stress and inflammatory reaction in rats with traumatic brain injury based on Nrf2/HO-1 signaling pathway. *China Pharmacy*, *34*(20), 2490-2496.
- Zhu, H., Yoshimoto, T., Imajo-Ohmi, S., Dazortsava, M., Mathivanan, A., & Yamashima, T. (2012). Why are hippocampal CA1 neurons vulnerable but motor cortex neurons resistant to transient ischemia? *Journal of neurochemistry*, 120(4), 574-585.